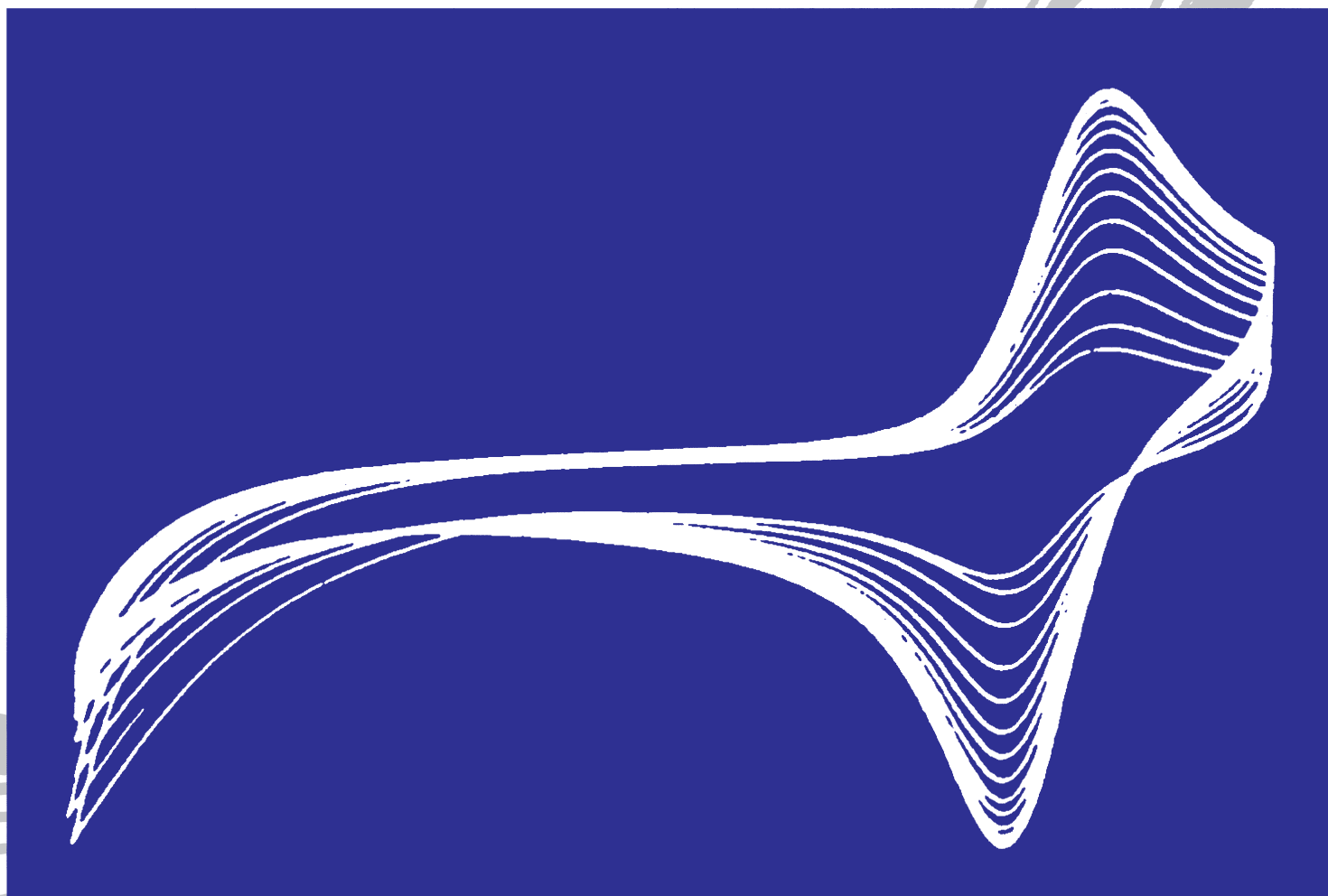


ELECTROANALYSIS

An International Journal Devoted to Fundamental and Practical Aspects of Electroanalysis



REPRINT

 WILEY-VCH

Full Paper

Metrological Aspects of Glucose Measurements by Biosensors

Samuel Wunderli, Hanspeter Andres*

Federal Office of Metrology METAS, Lindenweg 50, CH-3003 Bern-Wabern, Switzerland

*e-mail: hanspeter.andres@metas.ch

Received: January 14, 2009

Accepted: April 1, 2009

Abstract

In a chronoamperometric measurement the chemical activity of glucose is directly determined using a glucose sensitive biosensor based on glucose oxidase and an efficient mediator. Within the physiological range of 2 mmol kg⁻¹ and 10 mmol kg⁻¹ glucose in aqueous solutions behaves almost ideally and the chemical activity equals the glucose molality, the amount of glucose per unit mass of water, within the estimated measurement uncertainty. In physiological samples the equality between chemical activity and glucose molality is destroyed and has to be corrected for. Gravimetrically prepared mixtures of high purity glucose in buffered aqueous solutions are used as standards for calibration of the chronoamperometric measurement setup. Based on the model equation for the measurand aqueous or physiological sample, all significant sources of uncertainty are identified, their magnitude estimated from published and experimental data and finally combined to give the uncertainty in the reported value of the glucose molality. It is found, that the combined uncertainty of the glucose molality comprises mainly uncertainty contributions from the nonideal behavior, the chronoamperometric measurement setup, from the purity of glucose used and from the chemical composition of the test sample. The expanded uncertainty is below 2% rel., the glucose content determined by the bioelectrochemical measurements thus competes well with today's considered most accurate reference method Isotope Dilution Mass Spectrometry. Advantageous of the presented electroanalytical method is the direct measure of the glucose molality without prior sample preparation and dilution.

Keywords: Biosensors, Glucose oxidase, Standards, Metrology, Uncertainty, Traceability, Medicinal chemistry

DOI: 10.1002/elan.200904625

Presented at the International Conference on Electrochemical Sensors Mátrafüred 2008

1. Introduction

The European Community In Vitro Diagnostics Directive (EC IVDD) [1] states that "The traceability of values assigned to calibrators and/or control materials must be assured through available reference measurement procedures and/or available reference materials of a higher order". The EC IVDD triggered the formation of a Joint Committee for Traceability in Laboratory Medicine (JCTLM) by the Bureau International des Poids et Mesures (BIPM), the International Federation of Clinical Chemistry and Laboratory Medicine (IFCC) and the International Laboratory Accreditation Cooperation (ILAC) to meet the need of a worldwide platform to promote and give guidance on internationally recognized and accepted equivalence of measurements in laboratory medicine and traceability to appropriate measurement standards. The traceability of a measurement result, its link through an unbroken chain of comparisons to a reference standard, has become a key issue in the clinical chemistry field [2–5]. The JCTLM has established two working groups: WG1 deals with the identification and listing of reference materials and reference measurement procedures. The task of WG2 is to provide lists of reference measurement service providers who fulfill specified requirements prescribed by the JCTLM

[6]. Based on its legal mandate and the initiative of U. E. Spichiger-Keller (ETHZ) [7], the Federal Office of Metrology METAS (the Swiss national metrology institute) is building up a laboratory infrastructure for electroanalytical chemistry to provide a valuable contribution to the traceability of glucose content measurements by biosensors and ion activity measurements [8].

In human beings, glucose is the basic feed component for the cellular metabolism to mainly produce energy. The blood circulation supplies cells with glucose. A surplus of glucose can cause severe damage to the organism and can thus lead to major diseases, such as diabetes mellitus and its consequences. The measurement of blood glucose levels is therefore one of the most common tasks of a clinical chemical laboratory. Various types of instruments detect and report fundamentally different glucose quantities. In the clinical chemistry laboratory routine glucose measurements are primarily performed by photometry based on the absorbance of molecules involved in the enzymatic conversion of glucose in diluted samples. Results are reported as glucose concentration, amount of glucose per volume of specimen. In the reference photometric method D-glucose is selectively converted by the enzymes hexokinase and glucose-6-phosphate dehydrogenase to 6-phosphogluconate, whereas the coenzyme NADP is reduced to NADPH.

The absorbance of NADPH is measured in the UV region between 334 nm and 365 nm and is an indirect measure for the glucose concentration in the specimen [9]. Today, the most accurate reference method for glucose measurements is considered to be the isotope dilution technique using mass spectrometry (IDMS) [10, 11]. Through the addition of a well known amount of a uniformly labeled $^{13}\text{C}_6$ -isotope of glucose, glucose measurements of a rather high accuracy are feasible ($U = 1\text{--}2\%$, 95% confidence interval). Glucose standards are available either as pure materials or frozen human serum with a glucose concentration in the physiological range (2 mmol L^{-1} to 20 mmol L^{-1}). Self-monitoring and point-of-care testing devices use direct reading biosensors that do not need prior dilution of the test sample. They respond to (active) glucose molality, the amount of glucose per unit mass of water. The quantity molality is identical in whole blood, plasma or aqueous solutions. But, for concordance with traditional methods, the results are converted to concentration. This quantity now depends on the water content, which is different for whole blood (0.84 kg/L), plasma (0.93 kg/L) and aqueous solutions ($0.90\text{ kg/L} - 0.99\text{ kg/L}$) [12]. The IFCC therefore recommends reporting result for blood glucose always as concentration of glucose in plasma [13–15]. A fixed factor of 1.11 converts the concentration of glucose in whole blood to the equivalent concentration in plasma. For aqueous solutions the factor is between 0.94 and 1.03. These factors apply only to specimen with hematocrit, protein and lipid levels within their reference intervals. Misinterpretation or omission of these conversion factors in the calibration of glucose monitors with concentration standards can thus lead to false positive or false negative measurement results [16].

In this work we present a calibration method for glucose measurements without the need of prior dilution of the specimen. Chronoamperometric measurement signals of a glucose sensitive biosensor based on glucose oxidase and a mediator that prevents the formation of hydrogen-peroxide are used as the direct measure of the active glucose molality. Mediated chronoamperometric measurements of glucose contents in aqueous and physiological solutions have already been extensively described in the literature [17]. This

work focuses on the metrological aspects of such a quantitative electroanalytical measurement method. Up to now, neither a thorough uncertainty evaluation of chronoamperometric measurements results of glucose contents has been done nor has their traceability to internationally recognized standards been established. Highly reproducible amperometric measurements of gravimetrically prepared aqueous glucose standards in a fully automated flow system are used to do so. Test samples are either aqueous or physiological solutions.

2. Experimental

2.1. Amperometric Flow Setup

The amperometric sensor is a three-electrode device mounted in the fully automated flow system depicted in Figure 1. The flow cell made from polysulfone and the three electrodes were supplied by C-CIT (Wädenswil, Switzerland). The working electrode is composed of platinum contacted glucose sensing paste. The paste consists of glucose oxidase (GOD), the mediator system tetrathiafulvalene – *p*-tetracyanochinodimethane (TTF-TCNQ) and graphite suspended in silicone-oil. The application of the conductive organic salt TTF-TCNQ as a mediator for biosensors has been demonstrated [18] and recently reviewed [19]. To prevent depletion of the water soluble GOD during operation the paste is protected by a $20\text{--}50\text{ }\mu\text{m}$ cellulose cut open tubular membrane (Orange Scientific, Braine-l'Alleud, Belgium). The reference electrode is a closed system Ag/AgCl gel-type reference electrode. The counter electrode is simply a platinum wire. The current between the working and counter electrode after applying a constant voltage between the working and reference electrode is measured with a REF-0600 Potentiostat (GAMRY Instruments, Warminster, US). For variable temperature measurements the three electrode device was mounted into a B15 incubator (Heraeus, Hanau, Germany). The flow system is equipped with a peristaltic pump with twelve rollers Reglo Digital ISM 597 (ISMATEC, Glatt-

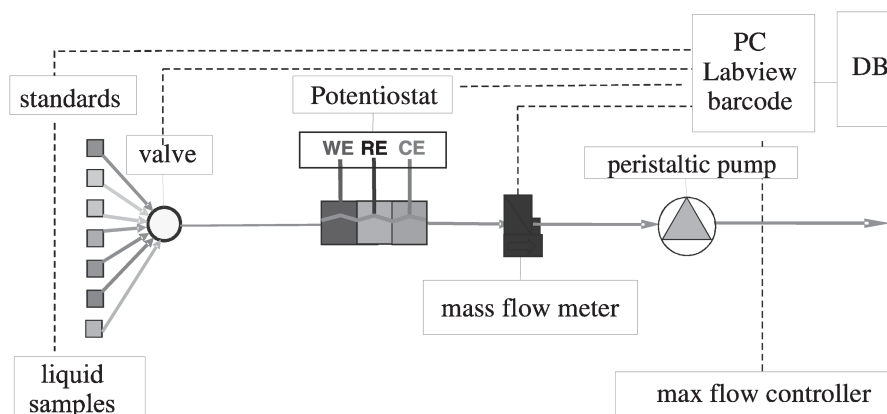


Fig. 1. Schematic view of the fully automated amperometric flow system at METAS equipped with flow cell and electrodes from C-CIT (WE: working electrode, RE: reference electrode, CE: counter electrode, and DB: database).

Table 1. pH, ionic strength I and glucose molality m of the buffered glucose standards and test samples are summarized. The uncertainty calculation for the glucose molality includes uncertainty contributions of the weighing data and environment as well as of the glucose purity.

Name	Buffer type	pH	Ionic strength I (mmol kg ⁻¹)	Glucose molality m (mmol kg ⁻¹)	Uncertainty u_m	
					(mmol kg ⁻¹)	(%)
I1	Imidazole	7.2	156.788	2.761	0.015	0.53
I2	Imidazole	7.2	157.216	11.324	0.028	0.25
I3	Imidazole	7.2	156.795	5.650	0.022	0.38
I4	Imidazole	7.2	156.794	8.446	0.025	0.29
I6	Imidazole	7.7	148.623	5.465	0.018	0.33
I7	Imidazole	6.7	166.738	5.372	0.018	0.34
I9	Imidazole	7.2	238.290	≈ 5.5		
P1	Phosphate	7.2	130.611	2.747	0.015	0.53
P2	Phosphate	7.2	130.611	11.271	0.028	0.25
P3	Phosphate	7.2	130.611	5.497	0.021	0.39
P4	Phosphate	7.2	130.611	8.298	0.025	0.30
P6	Phosphate	7.5	128.021	5.479	0.018	0.33
P7	Phosphate	6.5	132.473	5.459	0.018	0.33
P9	Phosphate	7.2	211.035	≈ 5.5		

brugg, Switzerland), a digital liquid mass flow meter ASL 1430-16 (SENSIRION, Staefa, Switzerland), two electric valve drives K-6 (KNAUER, Berlin, Germany), several NTC-type temperature sensors, an absolute pressure sensor 700–1200 mbar, humidity sensor, all of them connected to an Almemo 2890-9 instrument (AHLBORN, Holzkirchen, Germany), a max-flow controller and bar code reader (INETRONIC, Zollbrück, Switzerland). All components are controlled by a versatile LabView-program written by Heinz Herren (ISET, Laupen, Switzerland) including data storage of the results in a SQL-Lite database. The liquid test samples and standards are sucked in from bottles made of borosilicate glass closed with GL45 caps equipped with Teflon tube fittings and filter valves. All tubes are made of polytetrafluorethylene (PTFE) with 0.8 mm inner diameter (OMNIFIT, Cambridge, UK).

2.2. Glucose Standards

A standard for glucose measurements is a buffered and sterilized aqueous glucose solution of known molality. In the present work either imidazole or phosphate buffers in the pH range 6.7–7.7 were used. The pH of 100 mM imidazole (Fluka puriss p.a., Buchs, Switzerland) buffer solutions was adjusted by adding hydrochloric acid (37% HCl, Merck pro analysi, Darmstadt, Germany). To obtain an ionic strength in the physiological range the respective amount of lithium-chloride (Fluka puriss p.a., Buchs, Switzerland) was added. The pH of 50 mM disodiumphosphate (Fluka puriss p.a., Switzerland) buffer solutions was adjusted by adding hydrochloric acid (37% HCl, Merck pro analysi, Germany). Salt addition was obsolete as the ionic strength already lies in the required physiological range. Fouling of the buffered aqueous stock solutions is prevented by adding approx. 5 mM sodium azide (Fluka > 99%, Switzerland). Ultrapure water for dilution was obtained from an ELGA Puralab-

ultra unit (Labtec, Wohlen, Switzerland) feed by deionized water from the in-house system. Subsequently high purity glucose (Ferro Pfansteel, D112-1, Dextrose AC, anhydrous, US) is added to aliquots of the buffer solutions on the high precision balance Mettler XP-2004S (Mettler Toledo, Greifensee, Switzerland). Oligosaccharide impurities of the glucose were assessed by high performance liquid chromatography and the water content of the glucose was determined by Karl-Fischer coulometry. The purity of the glucose was determined as 99.7% ± 0.4% ($k = 2$, 95% confidence interval). The purity value corresponds to the SRM 917b from the National Institute of Standards and Technology (NIST), where the purity of D-glucose from the same manufacturer has been determined to a lower uncertainty of 0.2% ($k = 2$, 95% confidence interval). From the air buoyancy corrected weighing data and the determined purity the glucose molality of the standards is calculated. The relevant data of all standards and two test samples used in this study are summarized in Table 1.

2.3. Theory

Glucose oxidase is often used in direct reading biosensors to determine glucose enzymatically, a process during which the chemically active form of β-D-glucose is transformed highly selectively into 5-gluconolactone. Two electrons are released for each converted glucose molecule and mediated to the platinum electrode at a constant potential. This electron stream is the evaluable measuring signal in chronoamperometry and is directly proportional to the glucose content of the sample under test [20]. The Cottrell equation describes the relation between the diffusion limited current I and the glucose content at a planar electrode when a constant potential is applied: [21]

$$I = nAFa_S (D_S/\pi t)^{1/2} \quad (1)$$

n is the number of released electrons, A is the geometric surface of the planar electrode, a_S is the chemical activity of the substrate glucose, D_S is the diffusion coefficient of the substrate glucose, t is the time after applying a constant potential and F is the Faraday constant. Deviations from the Cottrell behavior occur at long times as a result of natural convection effects. When using microelectrodes this time drops below 1 s due to large radial diffusion contributions [22]. The latter case is applicable for the flow through system with a working electrode dimension of approx. 1 mm². After the formation of a constant Nernst diffusion layer with thickness δ_N at time t_1 the limiting current I_1 turns proportional to the substrate activity:

$$I_1 = nAFa_S D_S \delta_N^{-1} = K_S a_S \quad (2)$$

In this work Equation 2 is extended by a dynamic term $\kappa(t)$ and a drift term $D(t)$ as shown below:

$$I_1 = \kappa(t) K_S a_S + D(t) = \kappa K_S a_S + D \quad (3)$$

The term $\kappa(t) = \kappa$ mimics the response behavior of the biosensor in function of the time after a sample change. The term $D(t) = D$ accounts for a slow signal drift due to a sensitivity decrease of the biosensor.

The quantification of the uncertainty is done according to the principles outlined in GUM [23]. The combined uncertainty of the potential signal result from Equation 3 is equal to the positive square root of the combined variance $u_c^2(I_1)$, which is given by:

$$u_c^2(I_1) = \sum_{i=1}^N \left[\frac{\partial I_1}{\partial x_i} \right]^2 u^2(x_i). \quad (4)$$

Covariances are not considered in our approach at present. The standard uncertainties $u^2(x_i)$ of each influence X_i are either of the A- or B-type. A-type uncertainties can be evaluated from statistical distribution of the results of a series of measurements, while B-type uncertainties are evaluated from assumed a priori probability distributions based on experience, and from other information originating from separate experimental results.

3. Results and Discussion

3.1. Uncertainty Evaluation Using Buffered Aqueous Glucose Samples

In Figure 2 the chronoamperometric response signal I of a glucose sensitive electrode during the course of a fifty hour experiment at 23 °C is depicted. The applied voltage was 200 mV with a variance of 12 μ V during the experiment. A voltage of 200 mV proved optimal regarding high sensitivity and low background current. The measuring system was calibrated by alternating the glucose standards I1, I2, I3, I4,

I1 and P1, P2, P3, P4, P1, respectively. For each buffer type two independent calibrations were performed. The samples I9 and P9 were treated as unknown test samples and measured in between the respective system calibration. After each solution change the system was flushed with the subsequent solution for two minutes at a maximal flow rate of 1.5 mL min⁻¹. During these flushing periods spikes are observed in the current response. Throughout the experiment a zero sample flow was chosen to avoid possible flow currents, to save sample volume, and as no dependence of the measurement signal on the flow rate has been found. The measurement interval is two hours per sample.

The observed current varies in the range of 100 nA to 500 nA, depending on the glucose content of the sample under test. Thus, within two hours only the negligible amount of 1×10^{-13} to 4×10^{-13} mmol of glucose is converted to 5-gluconolactone at the working electrode. With an estimated sample volume of 0.5 mm³ around the working electrode the glucose content remains practically constant; the change is less than 1 μ mol kg⁻¹. As depicted in Figure 2 only a very small linear drift of approx. 2 nA/24 h is observed. Typically the signal reaches a steady state after an hour of measurement of a new sample. For the samples I9 and P9 the response behavior is different; after a decrease of the signal within the first hour the current increases again towards the end. This behavior is attributed to the reference electrode, which stabilizes much later due to the different ionic strength of the samples (see Table 1). Clearly, for the test sample P9 the steady state is reached at a latter time than for the test sample I9. For the subsequent signal analysis the last 100 s before a sample change are used to determine the limiting current I_1 . The mean experimental values of I_1 for the four measurement cycles depicted in Figure 2 are

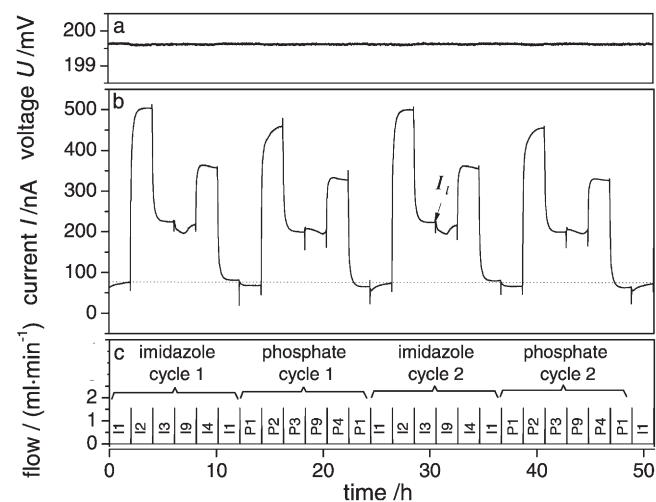


Fig. 2. A fifty hour chronoamperometric experiment is shown. a) Measured applied voltage U between working and reference electrode. b) Measured resulting current I between working and counter electrode. The limiting current value I_1 for the standard I3 in the imidazole cycle 2 is marked. The broken line visualizes a small linear signal drift $D(t)$ for the standard I1. c) Measured flow rate displaying the sample changes within the two measurement cycles of the imidazole and phosphate buffer system, respectively.

Table 2. Mean experimental values of current I_1 are summarized for two measurement cycles of the imidazole and phosphate buffer system, respectively. The respective standard deviations $s(I_1)$ are given in brackets.

Sample	Imidazole cycle 1 current I_1 (nA)	Imidazole cycle 2 current I_1 (nA)	Sample	Phosphate cycle 1 current I_1 (nA)	Phosphate cycle 2 current I_1 (nA)
I2	503.1(4)	499.3(3)	P2	460.3(3)	455.1(4)
I3	224.9(2)	222.7(2)	P3	199.2(2)	199.2(1)
I9	217.3(4)	215.6(2)	P9	201.0(9)	203.1(6)
I4	357.1(5)	355.4(2)	P4	327.3(1)	326.1(2)
I1	81.2(2)	80.1(3)	P1	65.4(1)	63.9(1)

summarized in Table 2. In the analysis only the value of the standards I1 and P1 at the end of each cycle were taken into account.

The different limiting current values in the cycles 1 and 2 for both buffer types are due to the above mentioned linear drift and can be compensated for mathematically.

The uncertainty budget for the response signal I_1 of the sample I2 and P2, respectively, is listed in Table 3. The mathematical expressions of the derivatives in Equation 4 are given together with typical values x_i for all influences X_i of the model Equation 3. The standard uncertainty for the chemical activity of $0.2\% \cdot a_S$ is derived as follows. For glucose in the physiological range of 2 mmol kg^{-1} to 10 mmol kg^{-1} the chemical activity corresponds virtually to the glucose molality. The deviation from the ideal behavior at 20°C is maximally 0.2% of the glucose activity [24–27]. The activity coefficient γ of the neutral glucose varies between 1.0003 and 1.0018. The activity coefficient is higher than 1 as the water activity decreases due to binding of water to glucose. At higher temperatures the differences between the two quantities glucose activity and molality gets

smaller [28]. The influence of the glucose purity is already included in the uncertainty of the glucose molality standards in Table 1 and therefore neglected in the uncertainty of the chemical activity. The A-type uncertainties of K_S , κ and D are taken from the experimental data depicted in Figure 2 and are summarized in Table 3. The proportionality factor K_S converts glucose activity to current and its uncertainty is given by the standard deviation of the limiting current $s(I_1)$ divided by the glucose activity, it is $0.5 \text{ nA } a_S^{-1}$ at maximum for the imidazole buffered solutions and $1.0 \text{ nA } a_S^{-1}$ for the phosphate buffered solutions. The uncertainty of the term κ is varied between 0‰ and 0.5‰. The uncertainty in the drift term D is simply the variance of the current $s(I_1)$. Again, it is estimated to be 0.5 nA and 1.0 nA for the imidazole and phosphate buffered solutions, respectively.

The resulting current I_1 together with its combined uncertainty $u(I_1)$ is given in Table 4. Results are shown for four varied values of $u(\kappa)$.

For a value of $u(\kappa) = 0.00$ an uncertainty of 1.1 nA and 1.7 nA results for the measured current I_1 of standard I2 and P2, respectively. All three uncertainties $u(a_S)$, $u(\kappa)$ and $u(D)$

Table 3. Uncertainty budget of the standards I2 (imidazole buffer) and P2 (phosphate buffer) in cycle 1 are listed.

Influence X_i	Sensitivity factor $[\partial I_1/\partial x_i]$	Typical values x_i	Uncertainty	
			$u(x_i)$	Type
a_S	κK_S	I2: $a_S = m_S = 11.301 \text{ mmol kg}^{-1}$ P2: $a_S = m_S = 11.249 \text{ mmol kg}^{-1}$	$0.002 a_S$	B
K_S	κa_S	I2: $44.428 \text{ nA (mmol kg}^{-1})^{-1}$ P2: $40.839 \text{ nA (mmol kg}^{-1})^{-1}$	I2: $0.5 \text{ nA } a_S^{-1}$ P2: $1.0 \text{ nA } a_S^{-1}$	A
κ	$K_S a_S$	1.000	$u(\kappa_1) = 0.000$ $u(\kappa_2) = 0.001$ $u(\kappa_3) = 0.002$ $u(\kappa_4) = 0.005$	A
D	1	0.00 nA	I2: 0.5 nA P2: 1.0 nA	A

Table 4. Measured current I_1 and combined uncertainty $u(I_1)$ for the standard I2 and P2, respectively, are listed as a function of the uncertainty of the dynamic term κ .

Sample		$u(\kappa_1) = 0.000$	$u(\kappa_2) = 0.001$	$u(\kappa_3) = 0.002$	$u(\kappa_4) = 0.005$
I2	I_1 (nA)	503.1	503.1	503.1	503.1
	$u(I_1)$ (nA)	1.1	1.3	1.50	2.8
P2	I_1 (nA)	460.3	460.3	460.3	460.3
	$u(I_1)$ (nA)	1.7	1.7	1.9	2.9

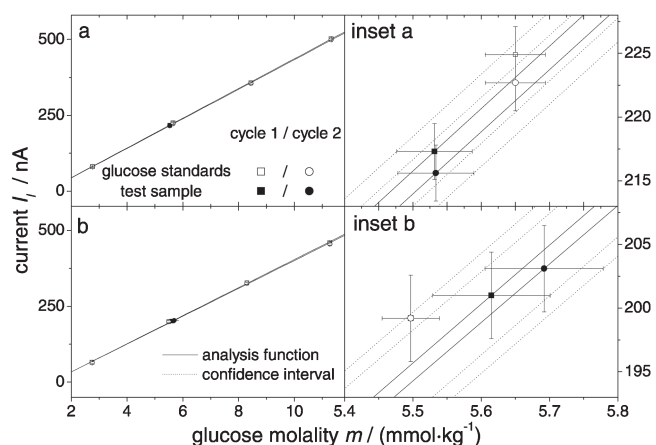


Fig. 3. Calibration functions with four glucose standards (open symbols) and one test sample (full symbols) are depicted. a) and Inset a) standards I1, I2, I3, I4, test sample: I9, b) and Inset b) standards P1, P2, P3, P4, test sample: P9. The analysis function is the inverse of the calibration function. From the depicted analysis function (full lines) with 95% confidence interval (dotted lines) the unknown glucose activity of the test samples and their respective uncertainties can be mathematically determined.

contribute to the combined uncertainty, the latter two dominate with 35.1% each for the standard P2. For the maximal uncertainty of $u(\kappa)$ the uncertainties of the limiting current I_l increase to 2.8 nA and 2.9 nA for the standard I2 and P2. Now, the uncertainty of I_l is dominated by the uncertainty of the dynamic term κ .

The glucose activity for the test samples I9 and P9, respectively, is determined as follows. From the glucose molalities of the standards I1, I2, I3, I4, P1, P2, P3 and P4 in Table 2 and the measured limiting current values of the standards and the two test samples I9 and P9, the glucose molality can be determined using the bracketing technique with a linear regression according to ISO standard 6143 [29]. In this type of linear regression both the uncertainty in the glucose molalities as well as the uncertainty in the measured currents are taken into account [30]. The calibration and analysis functions are depicted in Figure 3 assuming no uncertainty in the dynamic term κ . The resulting values for

glucose activity of the samples I9 and P9 are summarized in Table 5.

The values determined are concordant between the two measurement cycles and buffer systems, as can be seen from Figure 3 and Table 5. Concordance is already achieved assuming zero uncertainty in the dynamic term κ for both buffer types. For the imidazole buffered test sample I9 the glucose activity can thus be determined with a combined uncertainty of 0.5% rel. For the phosphate buffered test sample P9 the combined uncertainty is 0.8% rel.

3.2. Uncertainty Evaluation Using Physiological Samples

Buffered aqueous glucose standards allow the direct calibration of the amperometric flow system described in Section 2.1. Trough their gravimetric preparation traceability of chronoamperometric measurement results to the national realization of the international system (SI) is achieved. In the uncertainty evaluation of Section 3.1 the sample solution and the glucose standards were of the same aqueous type. When this approach is expanded to the measurement of physiological samples further uncertainty contribution of chemical and physical influences have to be considered and quantified.

Chemical influences include the difference in the chemical composition, pH and ionic strength of the sample solutions compared to the buffered aqueous glucose standards. As the glucose-oxidase based biosensor is highly selective towards glucose; varying chemical compositions do not affect the measurement result chemical activity of glucose. Thus, no correction of the glucose activity for changing chemical compositions is necessary. Still, the equality of chemical activity and glucose molality disappears due to binding of water to plasma proteins: e.g. in a physiological sample the protein level is between 68 g L⁻¹ and 72 g L⁻¹, that decreases the free water content by 30% of the protein level [31, 32]. Thus, the glucose molality is 2% lower than the measured chemical activity. The uncertainty of the glucose molality increases by 0.1% rel., when assuming a B-type uncertainty contribution of the free water content of 5% rel. The effect of a pH-change between sample solutions and standards is depicted in Figure 4. The

Table 5. Glucose activities a and uncertainty $u(a)$ of the test samples I9 and P9 for uncertainties in the dynamic term κ of 0.000 and 0.005 are listed.

	I9		P9	
	$u(\kappa_1) = 0.000$	$u(\kappa_4) = 0.005$	$u(\kappa_1) = 0.000$	$u(\kappa_4) = 0.005$
Cycle 1				
a (mmol kg ⁻¹)	5.531	5.53	5.615	5.61
$u(a)$ (mmol kg ⁻¹)	0.027	0.07	0.043	0.07
$u(a)$ (%)	0.5	1.3	0.8	1.2
Cycle 2				
a (mmol kg ⁻¹)	5.534	5.53	5.692	5.69
$u(a)$ (mmol kg ⁻¹)	0.027	0.07	0.043	0.07
$u(a)$ (%)	0.5	1.3	0.8	1.2

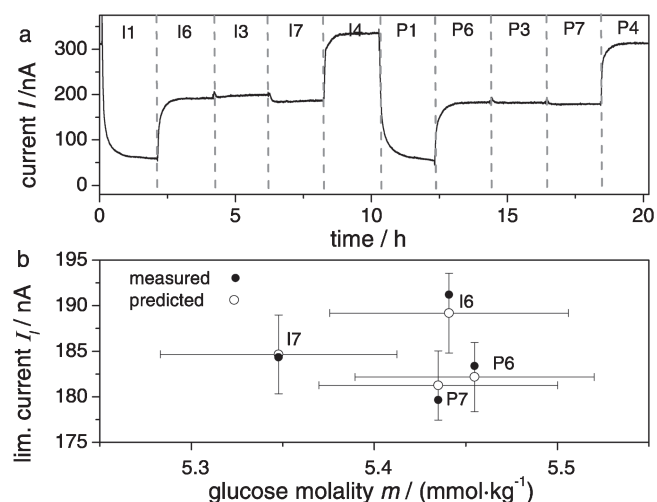


Fig. 4. A twenty hour chronoamperometric experiment at 23 °C is shown. a) Measured resulting current I between working and counter electrode. Measured standards are I1, I3, I4, P1, P3, and P4, respectively, with a pH 7.2. The intercalated test samples with varied pH-values are I6, I7, P6 and P7, respectively. The broken vertical lines represent the sample changes. b) Comparison of the measured (full circles) and predicted (open circles) limiting currents I_l . The analysis for the test samples I6, I7, and P6, P6 is based on the measurement results of the three standards I1, I3, I4, and P1, P3, P4, respectively.

pH of the sample solutions varies one pH unit (see Table 1). The predicted and measured limiting current I_l of the sample solutions agree well within their uncertainty. Thus, no correction of the glucose molality for the pH-variation in the physiological range is necessary.

Varying ionic strengths between the sample solutions and standards alter the response behavior of the amperometric flow system (see Fig. 2). The longer stabilization times are attributed to slowly changing liquid junction potentials at the interface reference electrode/sample solution [33]. Experimentally, this drawback is resolved by increasing the measurement times between sample changes or adjusting the ionic strength of the glucose standards to the sample solution. Thus, no correction of the glucose activity for varying ionic strength is necessary. Again, varied ionic strengths lead to a difference between chemical activity and glucose molality. The water activity changes due to binding of water to free ions: e.g., in a physiological sample the ionic strength varies between 145 mmol kg⁻¹ and 160 mmol kg⁻¹ water [34]. The glucose sample solutions I9 and P9 exceed these limits, possible effects are thus enhanced. In the physiological range the free water content differs maximally by 0.1% rel. Thus, the glucose molality differs maximally 0.1% from the measured chemical activity. Assuming a B-type uncertainty of the free water content of 0.05%, this uncertainty contribution to the glucose molality is negligible.

Typically, glucose measurements of physiological samples are done at 37 °C; the body temperature. The effect of the variable temperature measurements on the response of the amperometric sensor is shown in Figure 5. The temperature

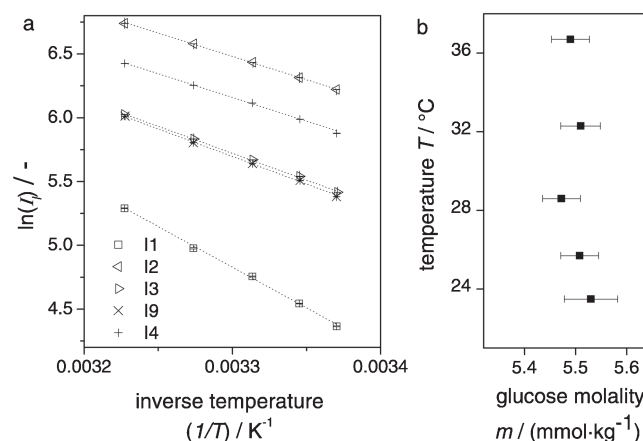


Fig. 5. Chronoamperometric measurement results of the imidazole buffered glucose standards I1, I2, I3, I4 and the sample solution I9 as a function of temperature are shown. a) An Arrhenius plot of the measured limiting current I_l . The dotted lines represent least squares fits. b) The predicted glucose molality m of the sample solution I9 as a function of temperature is compared. The analysis is based on the measurement results of the four standards I1, I2, I3, and I4.

behavior nicely follows Arrhenius. A least squares analysis results in activation energies in the range 30–50 kJ mol⁻¹; inversely proportional to the glucose molality. These activation energies correspond with the literature value of 41.1 kJ mol⁻¹ for immobilized glucose-oxidase at a glucose concentration of 1 mmol L⁻¹ [35]. The resulting glucose molality m for the sample solution I9 agrees well for variable temperature measurements between 23 °C and 37 °C. Thus, no correction of the glucose molality for variable temperatures is necessary. The considered chemical and physical influences have no effect on the measured chemical activity of glucose, but do alter the glucose molality. For the latter a correction for the water binding of plasma proteins is necessary; whereas the correction for water binding due to differences in the ionic strengths are negligible. These two corrections increase the expanded uncertainty at maximum by 0.3%, thus the expanded uncertainty is 1.3% rel. for the imidazole buffered test samples and 1.9% rel. for the phosphate buffered test samples.

4. Conclusions

Based on the model equation for the measurand, all significant sources of uncertainty of the analyte result are identified, their magnitude estimated from published and experimental data and finally mathematically combined to give the combined uncertainty in the reported value of the glucose molality. It is found, that the combined uncertainty of the glucose molality comprises mainly uncertainty contributions from the nonideal behavior, the chronoamperometric measurement setup and from the purity of glucose used and from the chemical composition of the test sample. The expanded uncertainty is below 2% rel. ($k=2$,

95% confidence interval) the glucose content determined by bioelectrochemical measurements thus competes well with today's considered most accurate reference method IDMS [10–11]. The advantage of the presented calibration method is its directness, the glucose content is determined without prior dilution of the sample. Furthermore, by restriction to the quantity molality no conversion factors for different specimens are needed as it is the case for concentration measurements.

5. Acknowledgements

The initiators of the project Prof. U. E. Spichiger and Dr. U. Feller are acknowledged for their decisive support and fruitful discussions. Heinz Herren from ISET GmbH Laupen receives a great thank for perfect Labview programming and consulting support for the potentiostat selection. O. Brunschwig, METAS mechanical and electronics support team as well as S. Spichiger from C-CIT Wädenswil are kindly acknowledged for their valuable support.

6. References

- [1] Directive 98/79/EC of the European Parliament and the council on in vitro diagnostic medical devices (p. 36), *Official Journal of the European Communities* **1998**, L331, 1.
- [2] M. L. Salit, T. Ciesiolka, N. Greenberg, R. R. Miller, W. G. Miller, G. L. Myers, M. Panteghini, G. Schumann, L. Siekmann, D. Sogin, *CLSI Publication, X5-R* **2006**, 26, 10.
- [3] L. Siekmann, *Accred. Qual. Assur.* **2004**, 9, 5.
- [4] K. Kuwa, K. Yasuda, *Anal. Sci.* **2001**, 17 (suppl.), i495-i498.
- [5] M. Panteghini, J. C. Forest, *Clin. Chim. Acta* **2005**, 355, 1.
- [6] L. Siekmann, *Accred. Qual. Assur.* **2006**, 11, 224.
- [7] U. E. Spichiger-Keller, *Chemical Sensors and Biosensors for Medical and Biological Applications*, Wiley-VCH, Weinheim, Germany **1998**.
- [8] S. Wunderli, H. Andres, *Electroanalysis* **2008**, 20, 324.
- [9] J. Neese, P. Duncan P, D. Bayse, M. Robinson, T. Cooper, *Clin. Chem.* **1974**, 20, 878.
- [10] D. Stöckl, H. Reinauer, *Clin. Chem.* **1993**, 39, 993.
- [11] L. Thienpont, A. P. Leenheer, D. Stöckl, H. Reinauer, *Clin. Chem.* **1993**, 39, 1001.
- [12] N. Fogh-Andersen, P. D. Wimberley, J. Thode, O. Siggaard-Andersen, *Clin. Chim. Acta* **1990**, 189, 33.
- [13] R. W. Burnett, P. D'Orazio, N. Fogh-Andersen, K. Kuwa, W. R. Külpmann, L. Larsson, A. Lewenstamm, A. H. J. Maas, G. Mager, U. Spichiger-Keller, *Clin. Chim. Acta* **2001**, 307, 205.
- [14] P. D'Orazio, R. W. Burnett, N. Fogh-Andersen, E. Jacobs, K. Kuwa, W. R. Külpmann, L. Larsson, A. Lewenstamm, A. H. J. Maas, G. Mager, J. W. Naskalski, A. O. Okorodudu, *Clin. Chem.* **2005**, 51, 1573.
- [15] P. D'Orazio, R. W. Burnett, N. Fogh-Andersen, E. Jacobs, K. Kuwa, W. R. Külpmann, L. Larsson, A. Lewenstamm, A. H. J. Maas, G. Mager, J. W. Naskalski, A. O. Okorodudu, *Clin. Chem. Lab. Med.* **2006**, 44, 1486.
- [16] J. Mahony, J. Ellison, *Clin. Chem.* **2007**, 53, 1122.
- [17] A. Chaubey, B. D. Malhorta, *Biosens. Bioelectron.* **2002**, 17, 441.
- [18] J. Müller, *Entwicklung eines modularen Durchflusssystems auf der Basis von amperometrisch-enzymatischen Biosensoren unter Verwendung von TTF-TCNQ als Mediator*. Dissertation, ETH, Zürich **2000**.
- [19] R. Pauliukaite, A. Malinauskas, G. Zhylyak, U. E. Spichiger-Keller, *Electroanalysis* **2007**, 24, 2491.
- [20] A. J. Bard, L. R. Faulkner, *Electrochemical Methods, Fundamentals and Applications*, 2nd ed., Wiley, Hoboken, USA **2001**.
- [21] F. G. Cottrell, *Z. Phys. Chem.* **1902**, 42, 385.
- [22] J. Wang, *Analytical Electrochemistry*, 2nd ed., Wiley, New York **2000**.
- [23] ISO/IEC Guide 98, *Guide to the expression of uncertainty in measurement (GUM)* **1995**.
- [24] K. Miyajima, M. Sawada, M. Nagagaki, *Bull. Chem. Soc. Jpn.* **1983**, 56, 1620.
- [25] Y. F. Hu, Z. C. Wang, *J. Chem. Thermodynamics.* **1997**, 29, 879.
- [26] J. Rösgen, B. M. Pettitt, D. W. Bolen, *Biochemistry* **2004**, 43, 14472.
- [27] J. Rösgen, B. M. Pettitt, D. W. Bolen, *Biophys. J.* **2005**, 89, 2988.
- [28] J. B. Taylor, J. S. Rowlinson, *Trans. Faraday Soc.* **1955**, 51, 1183.
- [29] ISO 6143, *Gas analysis – Comparison methods for determining and checking the composition of calibration gas mixtures*, **2001**.
- [30] A. Lybanon, *Am. J. Phys.* **1984**, 52, 22.
- [31] *Wissenschaftliche Tabellen Geigy*, Band 2, Ciba-Geigy AG, Basel **1979**.
- [32] M. K. Borisover, V. A. Sirotkin, B. N. Solomonov, *Thermochim. Acta* **1995**, 254, 47.
- [33] P. Henderson, *Z. Phys. Chem.* **1907**, 59, 118.
- [34] R. W. Burnett, A. K. Covington, N. Fogh-Andersen, W. R. Külpmann, A. Lewenstamm, A. H. J. Maas, O. Müller-Plathe, C. Sachs, O. Siggaard-Andersen, A. L. VanKessel, W. G. Zijlstra, *Clin. Chem. Lab. Med.* **2000**, 38, 1065.
- [35] M. Shaolin, K. Jinjing, *Electrochim. Acta* **1995**, 40, 241.